Smart Structures and Systems, *Vol. 19, No. 6 (2017) 625-631*
DOI: https://doi.org/10.12989/sss.2017.19.6.625

Cantilever beam vibration sensor based on the axial property of fiber Bragg grating

Miguel A. Casas-Ramos[*1] and G.E. Sandoval-Romero[2a]

[1]*Posgrado de Maestría y Doctorado en Ingeniería, Universidad Nacional Autónoma de México, Av. Universidad 3000 Edificio T "Bernardo Quintana Arrioja", 04510, México*
[2]*Centro de Ciencias Aplicadas y Desarrollo Tecnológico, Universidad Nacional Autónoma de México, Circuito Exterior S/N, A.P. 70-186, 04510, México*

(Received August 8, 2016, Revised May 15, 2017, Accepted May 22, 2017)

Abstract. In the fields of civil engineering and seismology, it is essential to detect and tracking the vibrations, and the fiber Bragg gratings (FBGs) are typically used as sensors to measure vibrations. Where, one of the most popular and detailed approaches to use FBGs as vibration sensors involves the use of cantilever beam designs, which adds a mass to measure low and moderate frequencies (from 20 Hz up to 1 kHz) with high sensitivities (greater than 10 pm/*g*). The design consists of a bending strain in the cantilever that is simultaneously transferred to the FBG, resulting in a shift in the wavelength that is proportional to the strain experienced by the cantilever. In this work, we present the experimental results of a vibration sensor design using a cantilever beam to generate an axial uniform strain in the FBG in-line with the vertical axis, which modifies the cantilever's natural frequency that allows the sensor to have a wide frequency broadband without losing sensitivity. This sensor achieved a sensitivity of about 339 pm/*g* and a natural frequency of 227.3 Hz. The presented design compared with the traditional cantilever beam-based FBG vibration sensors, has the advantages of a simple design for detection on vibration-sensitive structures and its physical parameters can be easily modified in order to satisfy the requirements of the desired vibration measurements.

Keywords: cantilever; fiber Bragg grating; frequency; sensitivity; vibration

1. Introduction

Different approaches and approximations have been used for cantilever-mass analyses and designs to determine the best way to improve the strain at the fiber Bragg grating (FBG). In simple beam designs, pure bending theory can be used to calculate the sensor behavior; an example of this approach was reported by Wang *et al*. (2013), who constructed a sensor with an effective natural frequency of 205 Hz by applying pure bending theory with temperature self-compensation. However, this sensor suffered from a low sensitivity of 10 pm/*g* (where *g* represents the gravitational acceleration of 1 g=9.81 m/s^2). Basumallick *et al*. (2012) enhanced the sensor's sensitivity without altering the pure bending analysis; this involved altering the distance between the axis of the FBG to the neutral axis of the cantilever beam, where a patch was placed between the beam and the FBG. This patch must have a Young's modulus lower than the beam material, such that the patch does not alter the beam behavior. The authors achieved a sensitivity of 450 pm/*g* and a resonance frequency of 12 Hz, and as most of the vibration sensors based on cantilever beam structures, this structural design can be easily implemented but its resonant frequency is low. In general, the sensitivity and repeatability of this kind of sensors are limited by gluing process of the FBG and a non-uniform surface strain distribution on the FBG.

In addition, in this field of research, many researchers have used an L-shaped rigid cantilever beam attached to a leaf spring design, which creates an air gap instead of using a patch to alter the distances between axes. This allows to use the axial property of a suspended FBG as an elastic element to measure vibration, and allowing to overcome the disadvantages of pasted FBG based accelerometers. An example of this change in the FBG location and the structure analysis, where the FBG was attached to the structure shell and the arm of the cantilever, was developed by Weng *et al*. (2011), which resulted in a configuration with a high sensitivity of 106.5 pm/*g* and provided a wide frequency response range of 0-110 Hz. This configuration has well balance specs, between a high sensitivity and a wide bandwidth. The implementation of the axial and transverse properties of a fiber optic takes advantages of the elastic properties of the fiber optics, improving the resonant frequency of the designs and the sensitivity. In order to improve the resonant frequency and the effective working bandwidth, Li *et al*. (2017) presented a diaphragm-based FBG vibration sensor, which uses the transverse property of a tightly suspended optical fiber with two fixed ends. This sensor had a linear response over a frequency ranging from 10~150 Hz and a resonant frequency of 300 Hz, however the vibration sensitivity is 31.25 pm/*g*. The use of two FBGs in their proposed sensor, allows to the sensor to

*Corresponding author, Ph.D. Student
E-mail: miguel.casas@ccadet.unam.mx
[a] Dr.
E-mail: eduardo.sandoval@ccadet.unam.mx

ISSN: 1738-1584 (Print), 1738-1991 (Online)

simultaneously measure the temperature and medium-high frequency vibrations (decoupling vibration and temperature), so the temperature response was decreased to 1.32 pm/℃ in the range of 30~90℃ (after implementing the temperature compensation).

From the cantilever analysis designs, it has been observed that the designs either have a high sensitivity or a wide broadband; the described analysis consists of a cantilever with a concentrated load at the tip of the beam, such that the beam should be treated as a volumetric solid with mass.

In this paper, we described the sensor's theoretical basis for the sensitivity and natural frequency enhancing of a cantilever mass based FBG sensor vibration, by placing the FBG at the maximum bending point, generating an axial uniform strain in the FBG in-line with the vertical axis, which modifies and increase the cantilever's natural frequency that allows the sensor to have a wide frequency broadband without losing sensitivity. An example of the use of axial property of the fiber optic to enhance the characteristics of the sensor is given by Li *et al*. (2017). They proposed an acceleration sensor based in the axial property of a tightly suspended fiber optic along with a diaphragm, in order to enhance the sensitivity, working bandwidth and the natural frequency of the sensor. Our present work provides a simple and more accurate approximation of the beam, as a non-uniform cantilever beam comprising two different solids (i.e., a beam and a block of mass), this non-uniform cantilever beam will strain the FBG uniformly along the fiber axis. In this paper, it is shown experimentally that using a FBG as a spring where the maximum bending occurs enhances the cantilever behavior, attaining a sensitivity greater than 300 pm/*g* (without degrading the transfer of strain from the cantilever to the FBG) and the resonant frequency of the structure is affected and increased to a value greater than 200 Hz. The described design exhibits a high sensitivity without sacrificing broadband performance.

2. Sensor measurement principle

Enhancing the sensor bandwidth and sensitivity with the vibrations involves markedly increasing the strain along the FBG without cracking it, which thereby increases the shift in the FBG reflected spectrum.

As reviewed in section 1, most of the vibration sensor designs have one aspect in common: the FBG is attached in parallel with the cantilever neutral axis and the cantilever's top face; this is done because this design hardly or does not alter the system analysis as a simple beam design that can be described by pure bending theory. However, this limits the options of sensitivity and the natural frequency because the cantilevers oscillate with low frequencies.

However, by placing the FBG where the maximum deflection occurs (at the tip of the non-uniform cantilever) due to the mass displacement from the vibrations and in line with the vertical axis (Fig. 1), the FBG will stretch uniformly. This change is not only related to the change in the grating period and therefore, the Bragg wavelength shift, with strain along the FBG caused by the vertical vibrations or accelerations, but also increases the Bragg wavelength shift. Additionally, this design also modifies the natural frequency of the cantilever.

2.1 FBG vibration sensor design

The sensor consists of a single piece that is fabricated with aluminum 7075, the inertial mass supported by a cantilever beam, and an FBG that is bonded perpendicularly between the mass tip and the sensor frame, Fig. 1(a). The cantilever beam with a non-uniform cross section (see Fig. 1) parameter are listed in Table 1. The FBG used as sensing element has a centered wavelength (λ_B) at 1549.622 nm, with a maximum reflectivity of 90.27%, and a FWHM (full width at half maximum) of 0.31 nm and a length of 12 mm.

The inertial mass moves along the vertical axis z with the external vibrations. A single vertical movement was likely caused by a small movement at the tip of the cantilever beam with non-uniform cross section; the fiber section with the FBG, which is bonded between the inertial mass tip and the frame, restrains the cantilever-mass movement. In addition, this restrained movement changes the cantilever beam's natural frequency due to the dependence of Young's modulus of the fiber. Because the FBG has an elastic behavior, being elongated and recovering its original form, under forces less than 20 N (Antunes *et al*. 2012). The FBG segment (considered as a segment of a prismatic bar of circular cross section) experience an elongation equals to its length divided by the total length L_3 and multiplied by the total elongation δ_A. This quantity is called the elongation per unit length, or strain, denoted by ε (Hibbeler 2006, Gere and Goodno 2009). The strain is given by the equation

$$\varepsilon = \frac{\delta_A}{L_3} \tag{1}$$

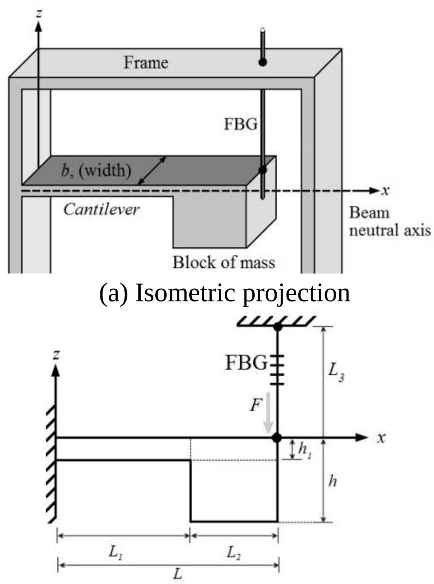

(a) Isometric projection

(b) Cross section

Fig. 1 Sensor schematics of the FBG accelerometer

Table 1 Parameters of the vibration sensor

Parameter	Value	Description
L_1	29.27 mm	Cantilever length
L_2	16.34 mm	Mass block length
L_3	19.43 mm	Length of the fiber attached between the cantilever's tip, and a fiber section containing the FBG
L	45.61 mm	Total length = L_1+L_2
h_1	1 mm	Cantilever height
h	24.53 mm	Mass block height
b	16.42 mm	Width of the cantilever and mass block
M	19.51 grams	Total effective mass
E_{AL}	72 GPa	Aluminum 7075 Young modulus

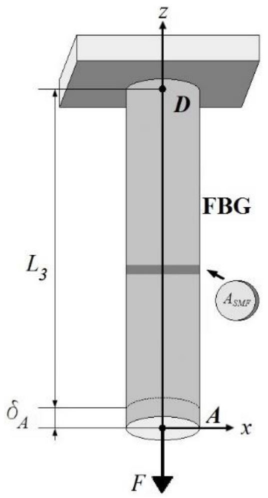

Fig. 2 Schematic for the FBG strain

2.2 FBG total elongation

The length elongated by the FBG (Fig. 2) is same as the total displacement due to the deflection of the cantilever beam at the point *A* (Fig. 1). The displacement at the cantilever tip (known as deflection) was calculated from the structure geometry, by applying the method of the superposition (Hibbeler 2006, Gere and Goodno 2009), Fig. 3(a), to each section of the cantilever beam with non-uniform cross-section (Fig. 1): the cantilever and mass block.

The first deflection represented with δ_1 due to bending of the beam part *AC* in Fig. 3(a) (mass block) shows that the mass block is held rigidly at point *C*, so it neither deflects nor rotates at that point. Since it has length L_2 at *AC* and its moment of inertia $I_1=(bh^3)/12$, the δ_1 deflection is given by

$$\delta_1 = \frac{FL_2^3}{3E_{AL}I_1} \tag{2}$$

In Fig. 3(a), due to the bending at the *CB* section of the cantilever and the contribution to the deflection at *A*. At the *C* point, this section is subjected to a concentrated load *F* with a moment FL_1 and an inertia moment $I_2=(bh_1^3)/12$. This results in a δ_2 deflection

$$\delta_2 = \frac{FL_1}{6E_{AL}I_2}\left(L_1\left(2L_1+3L_2\right)+3L_2\left(L_1+2L_2\right)\right) \tag{3}$$

The final deflection δ_A (seen in Fig. 3(b)) at the tip of the beam (point *A*) is equal to the sum of the deflections δ_1 Eq. (2) and δ_2 Eq. (3)

$$\delta_A = \delta_1 + \delta_2 = \frac{F\left(2L_2^3I_2 + I_1L_1\left(L_1\left(2L_1+3L_2\right)+3L_2\left(L_1+2L_2\right)\right)\right)}{6E_{AL}I_1I_2} \tag{4}$$

2.3 Estimating the characteristic sensor theoretical sensitivity and natural frequency

Maximum deflection occurs at the tip of the cantilever beam with non-uniform cross section caused by the vertical acceleration on the structure. This deflection was calculated by analyzing the structural geometry and applying the method of superposition (Eq. (4)), because the cantilever and the inertial mass are part of a single manufactured piece. Finally, the strain experienced along the FBG axis (given by Eq. (1)) depends on the cantilever displacement (Eq. (4)), which changes the original FBG length, and this is expressed as follows

$$\varepsilon = \frac{M\left(2L_2^3I_2 + I_1L_1\left(L_1\left(2L_1+3L_2\right)+3L_2\left(L_1+2L_2\right)\right)\right)}{6E_{AL}I_1I_2L_3}\cdot g \tag{5}$$

where g is the acceleration, and M is the effective mass of 19.40 grams for the cantilever beam with non-uniform cross section; L_1 is the beam length; L_2 is the block of mass length; L is the sum of the beam and the block of mass length; L_3 is fiber length section with the Bragg grating glued in the mechanical arrangement (as seen in Fig. 1); and E_{AL} is Young's modulus for the beam material.

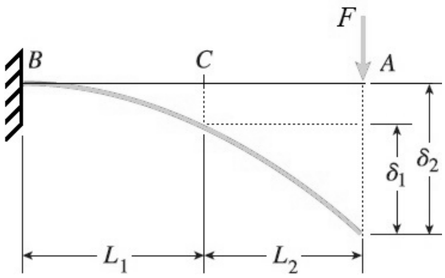

(a) Deflection due to bending of AC and CB parts of the beam

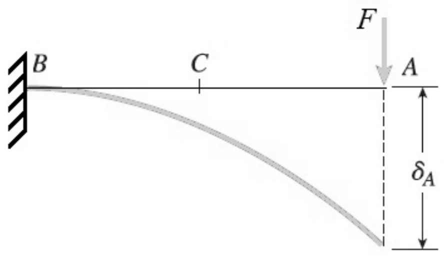

(b) Total deflection

Fig. 3 Cantilever beam superposition analysis

The change in the FBG position and location allows for a uniformly distributed strain along the FBG axis maximizes the Bragg wavelength shift, Fig. 1 shows the section of the fiber optic with the FBG placed and glued between the block of the mass tip and the sensor frame perpendicular to the non-uniform cantilever beam surface.

According to the Bragg's grating theory (Kersey *et al*. 1997 and Kashyap 2009), the wavelength shifts are caused by the strain and temperature fluctuations, these can be described in terms of the photo-elastic and thermo-optic effects, resulting in

$$\Delta\lambda_B = \lambda_B\left(1-P_e\right)\varepsilon + \left(\alpha+\zeta\right)\Delta T \tag{6}$$

where $\Delta\lambda_B$ is the wavelength shift of FBG; λ_B is the FBG central wavelength; P_e is the effective photo-elastic constant; ε is the axial strain; α is the thermal expansion coefficient of the fiber optic; ζ is the silica thermo-optic coefficient; and ΔT is the temperature change.

Because, the temperature in the test room were constant and the wavelength shifts due to the thermal effects occur much slower than the mechanical changes due to the acceleration. The thermal changes can be neglected from Eq. (6) and can be simplified as

$$\Delta\lambda_B = \lambda_B\left(1-P_e\right)\varepsilon \tag{7}$$

With the FBG oriented perpendicularly to the cantilever beam and knowing the mechanical behavior (strain ε) with the acceleration dependence described by Eq. (5), the ratio of the FBG wavelength shift in the reflected spectrum per acceleration unit, which is also called the sensitivity, is given by reference

$$S = \frac{\Delta\lambda_B}{g} = \lambda_B\left(1-P_e\right)\frac{\varepsilon}{g} \tag{8}$$

where the effective photoelastic coefficient *Pe* is relative to Poisson ratio and the effective refractive index core of the fiber optic (i.e., for an SMF-28e fiber optic, *Pe* is equal to 0.20, Bertholds and Dändliker 1988, Jülich *et al*. 2013). From Eq. (8) and the Table 1 parameters, the change in the Bragg wavelength with the gravitational acceleration of 1 *g* indicates that the sensitivity is equal to 386 pm/*g*.

Now, the Fig. 1 can be simplified to a mechanical first order degree system (mass-spring), Fig. 4. Where, the displacement of the cantilever from its average equilibrium position due to the acting vertical force, and it is necessary an expression to describe the system and the natural frequency for small amplitudes of vibration.

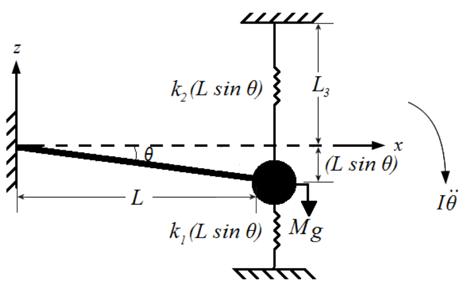

Fig. 4 Sensor's mechanical system of a single degree of freedom

The motion equation of the behavior is given by the D'Alembert's principle. This principle states that if a body is not in static equilibrium due to the acceleration it possess, the body can be brought to static equilibrium by introducing on it an inertia force which acts through the center of gravity of the body in the direction opposite to acceleration and is equal to mass times acceleration, Eq. (9). But from Figs. 1 and 5(b), it can be seen that the arrangement position of optical fiber do not pass the center of gravity of mass in the vertical direction (as seen in Fig. 4), which leads to a distance between optical fiber and center of gravity in the horizontal direction. However, this is not considered in the following Eq. (9), because it is very small and can be ignored.

$$ML^2\ddot{\theta} + \left[L^2\left(K_1+K_2\right)-FL\right]\theta = 0 \rightarrow \ddot{\theta}+\omega_n\theta = 0 \tag{9}$$

From (9) the sensor's undamped natural frequency can be written as follows (see Fig. 4)

$$f_n = \frac{1}{2\pi}\sqrt{\frac{\left(K_1+K_2\right)L^2-FL}{ML^2}} \tag{10}$$

where K_1=3220.13 N/m and K_2=40188.88 N/m are the cantilever beam and fiber optic spring constant, respectively; $L=L_1+L_2$; and $F=M\bullet g$. From Eq. (10), the sensor's calculated fundamental natural frequency is $f_n=\omega_0/2\pi$=237.4 Hz.

3. Experimental results

From section 2, it was stated that with a change in the FBG location and position, a high strain can be maintained and at the same time, can modify and increase the natural frequency. The sensor theoretical behavior was described, and the calculated values of sensitivity (which depends on the strain) and the natural frequency were obtained. Now, it is essential to evaluate the actual sensor performance to compare the predicted values against the actual values to demonstrate the enhancement in the essential parameters for these types of sensors: operation bandwidth, natural frequency and sensitivity.

First, it is necessary to measure the sensor frequency response range because this determines the possible applications for the sensor. To obtain the sensor's operational range, the experimental setup to test the response to the vibrations (see Fig. 5(a)) was established using a STEREN BOC-200 speaker placed below the sensor to induce vibrations (Fig. 5(b)); the frequency was changed using a function waveform generator driver (AGILENT 33521A), and the reflected response from the broadband source was measured using an OEMARKET PD-A-25 photodiode and a TEKTRONIX TDS3034C oscilloscope.

Fig. 6 shows the test results as the input signal frequency increased from 0.05 to 250 Hz with a gravitational acceleration of 1 *g* and an inertial mass of 18.69 grams; this test was repeated three times. Two primary linear behaviors are shown in Fig. 6: one at the slope of the frequency response from 0.05 to ~10 Hz (a range of 9.95 Hz), and the other from 10 Hz to 210 Hz (i.e., an effective operational range of 200 Hz). Those operational ranges are the ranges where the sensor can function with stability and with a known behavior.

Leaving the non-uniform cantilever beam to oscillate freely, the sensor's natural frequency can be obtained by applying the fast Fourier transform to the time-domain data. As shown in Fig. 7, the sensor frequency spectra were obtained, and these spectra allowed for the resonant identification of each data test. For seven independent tests, the observed measured mean natural frequency of the sensor prototype was 227.3 Hz, and based on Eq. (10), the natural frequency was 237.4 Hz; therefore, the test results correspond to a relative error of 4.4% with a repeatability error of 1.9%.

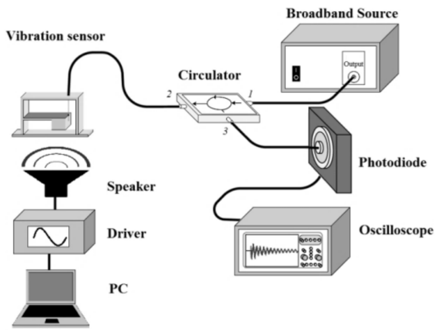

(a) Experimental schematic setup

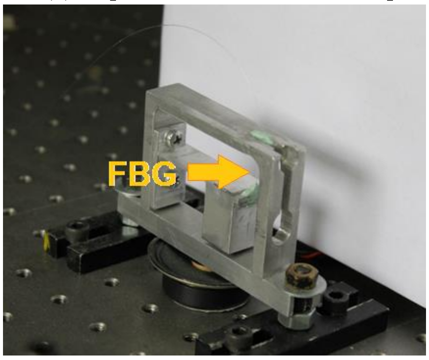

(b) Speaker placed below the sensor

Fig. 5 The sensor experimental setup with the amplitude-frequency curves, for the applied vibrations under the sensor

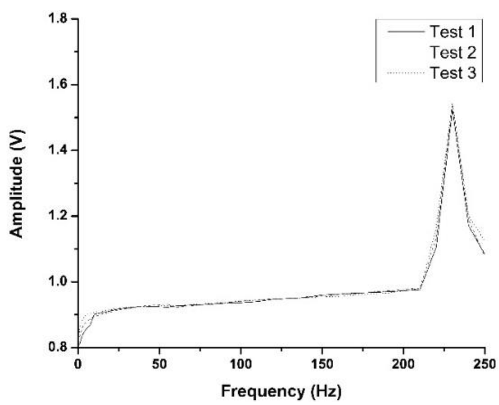

Fig. 6 Frequency-amplitude response curves for the sensor per test

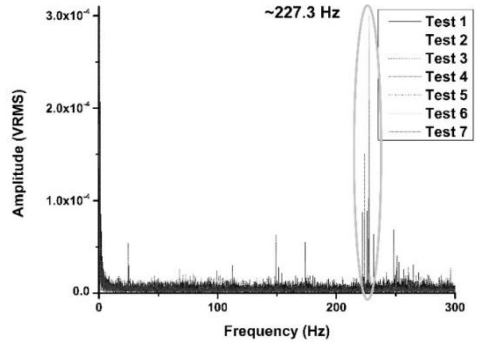

Fig. 7 Sensor's frequency FFT spectrum with the natural frequency peak locations per test

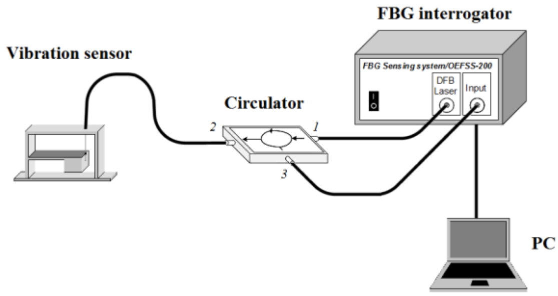

Fig. 8 Experimental setup used to measure the Bragg wavelength shift

The corroboration of the sensor operation bandwidth and natural frequency values (more than 200 Hz) with the predicted values is half of the challenge because it was demonstrated that a fiber optic with the FBG can be used as a spring due to its plastic behavior, which modifies the cantilever natural frequency.

Now, it is necessary to determine the sensor's characteristic sensitivity to demonstrate the second statement: a high sensitivity (>300 pm/g) without a low frequency. The experimental setup to measure the Bragg wavelength change uses an OELAND OEFSS-200 FBG interrogation unit (Fig. 8) with an accuracy of 2 pm and a resolution of 1 pm. With this setup, FBG wavelength shifts can be measured.

To measure the shifts, two measurement cycles were performed with four independent tests in each cycle. The first cycle considered the fiber optic with the FBG placed tense inside the mechanical arrangement with no bending in the cantilever, as seen in Fig. 1(a), and from Fig. 9(a) the mean measured Bragg wavelength equals to λ_{B1}=1549.630 nm with a repeatability of 98.9%. In the second cycle when the cantilever oscillates freely due to the gravitational acceleration (1 g) and there aren't any external vibration from BOC-200, the Bragg wavelength shifts positively (as seen in Fig. 9(b)) and the mean Bragg wavelength equals to λ_{B2}=1549.969 nm, and shows a repeatability of 95.2%.

The sensor's sensitivity using the interrogation unit equals the shift in the wavelengths between the cases with and without bending, resulting in a wavelength shift mean of $\Delta\lambda_B=\lambda_{B2}-\lambda_{B1}$=339 pm. The measured acceleration (in Fig. 10) was obtained from the Bragg wavelength displacements in Fig. 7 in absence of any external vibration from the BOC-200.

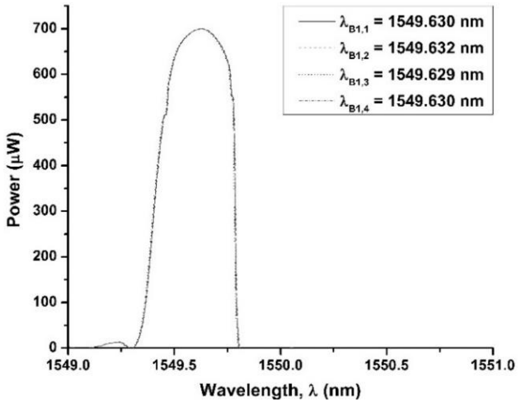

(a) Cantilever without bending

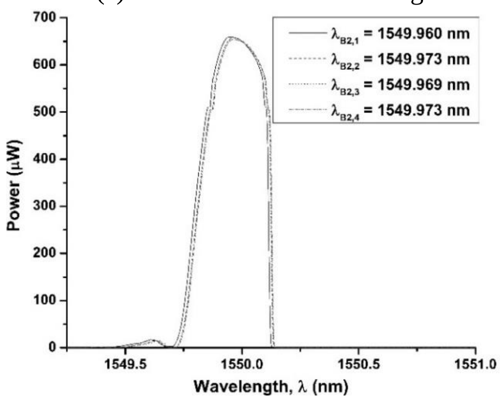

(b) Cantilever oscillating freely

Fig. 9 Reflected Bragg spectrum for the two fundamental sensor conditions

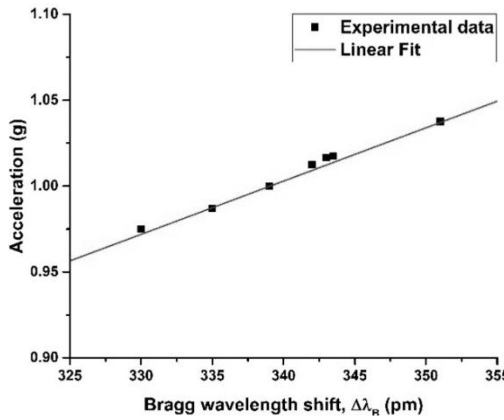

Fig. 10 Acceleration experienced by the sensor during the tests, due to the free vertical oscillations in Fig. 7

For the Fig.10, the equation of fitted line is given by $0.0031\Delta\lambda_B$-0.0511, with a R^2 value of 0.9914. The sensing properties are given by the data recorded with the free vertical oscillations from the cantilever. Such as an excitation about 1 *g* (a mean acceleration of $g=\Delta\lambda_B/S=1.006$ *g*) and by using an interrogator with a resolution of 1 pm (picometer), it was possible to measure a minimum acceleration of 0.003 *g* with a precision of 0.0015 *g*, with a sensitivity to the acceleration experience of S=339 pm/*g* and an effective operational frequency of 227.3 Hz near to the calculated resonance frequency of 237.4 Hz.

5. Discussion

A wide variety of vibration sensor designs that use a cantilever beam and a mass to modulate the fiber Bragg grating period through the strain in the FBG (i.e., along its axis) due to the bending of the beam have been documented. These designs allow for the measurement of low and moderate frequencies with a wide effective frequency operation range and a high sensitivity (the Bragg wavelength shift with the vibration experienced). For vibration sensors, strain is the only important parameter thus, some techniques or considerations have been made by several authors to eliminate or markedly decrease the FBG temperature dependence. To overcome this problem, the temperature inside the test room were kept stable so the FBG were exposed to a constant temperature. The temperature were monitored and the temperature changed by approximately 0.1℃, so these fluctuations should be minimized because the only important wavelength shifts are caused by the mechanical strain. However, the center wavelength shifts of this sensor due to the exposition to abrupt temperature changes will be analyzed and solved in future works.

Fig. 6 shows the test results from three different frequency sweeps using the BOC-200, these results indicates that the sensor works linearly within the frequency range of 10~210 Hz (the working bandwidth) and the amplitude reaches a maximum at 227.3 Hz (this represents the resonant frequency according to Eq. (10)). While Fig. 7 shows the frequency spectra data for seven tests, where the resonant frequency is about 227.3 Hz when the acceleration is at 1 *g*. This agrees with the calculated value of 237.4 Hz from Eq. (10); therefore, the test results correspond to a relative error of 4.4% with a repeatability error of 1.9%.

The experimental results demonstrate a linear response of the detected acceleration versus the wavelength shift (in Fig. 10) for 227.3 Hz, close to the resonance frequency of the FBG sensor, when the cantilever oscillates freely in absence of any external vibration from the BOC-200. With a sensitivity of 339 pm/*g* and a repeatability of 95.2%, which agrees with the theoretical analysis in Eq. (8).

6. Conclusions

In the work, it has been demonstrated that the sensor can measure (with an excellent linear response) vertical oscillating applied signals, which can capture input signals of less than 227.3 Hz, as seen in Fig. 3. This is corroborated in Fig. 4, where other frequency components were detected, such as workshops, people walking, and other experiments conducted near the laboratory.

When a vertical vibration is applied to the cantilever beam, the FBG is strained uniformly, and the reflected wavelength changes positively and linearly. In this study, a favorable experimental wavelength shift of 326 pm/*g* and an acceleration of 1.006 *g* were achieved, which led to the creation of a probe that uses the fiber optic with the FBG as a spring, which can not only enhance the cantilever natural frequency but can also linearly and uniformly strain the

Bragg grating to increase the Bragg wavelength shift.

However, the FBG was placed manually in this study, and the natural frequency and sensitivity could be improved by correcting the misalignment or correcting an error in positioning the FBG using an effective method to place the fiber for future tests.

The proposed system demonstrated an excellent performance and thus, it can be applied to on-site measurements and structural dynamic monitoring in civil engineering or seismic studies. With the demonstration of an excellent dynamic response for this device, the configuration can also reduce the sensor's dimensions, which would make it more portable and lighter.

Acknowledgments

This study was supported by DGAPA-UNAM through project IT101515. Miguel A. Casas-Ramos is grateful to CONACYT for the financial support in the form of a scholarship for the Master's and PhD Engineering Program through the Universidad Nacional Autónoma de México.

References

Antunes, P., Domingues, F., Granada, M. and André, P. (2012), *Mechanical Properties of Optical Fibers, Selected Topics on Optical Fiber Technology*, (Ed., Moh. Yasin), InTech. Available from: http://www.intechopen.com/books/selected-topics-on-optical-fiber-technology/mechanical-properties-of-optical-fibers (accessed 10.01.15)

Basumallick, N., Chatterjee, I., Biswas, P., Dasgupta, K. and Bandyopadhyay, S. (2012), "Fiber Bragg grating accelerometer with enhanced sensitivity", *Sensor. Actuat. A - Phys.*, **173**(1), 108-115.

Berkoff, T.A. and Kersey, A.D. (1996). "Experimental demonstration of a fiber Bragg grating accelerometer", *IEEE Photonics Technol. Lett.*, **8**(12), 1677-1679.

Bertholds, A. and Dändliker, R. (1988), "Determination of the individual strain-optic coefficients in single-mode optical fibres", *J. Lightwave Technol.*, **6**(1), 17-20.

Ferraro, P. and De Natale, A. (2002), "On the posible use of optical fiber Bragg grating as strain sensors for geodynamical monitoring", *Opt. Laser. Eng.*, **37**, 115-130.

Gere, J.M. and Goodno, B.J. (2009), *Mechanics of Materials*, (7th Edition), Cengage Learning, Toronto, Ontario, Canada.

Hibbeler, R.C. (2006), *Mecánica de materiales*, (6th Edition), Pearson Prentice Hall, Naucalpan de Juarez, Mexico.

Jülich, F., Aulbach, L., Wilfert, A., Kratzer, P., Kuttler, R. and Roths, J. (2013), "Gauge factors of fibre Bragg grating strain sensors in different types of optical fibres", *Meas. Sci. Technol.*, **24**(9), 1-7.

Kashyap, R. (2009), *Fiber Bragg Gratings*, (2nd Edition), Academic Press, Burlington, MA, USA.

Kersey, A.D., Davis, M.A., Patrick, H.J., LeBlanc, M., Koo, K.P., Askins, C.G., et al. (1997), "Fiber grating sensors", *J. Lightwave Technol.*, **15**(8), 1442-1463.

Li, K. (2016), "Review of the strain modulation methods used in fiber bragg grating sensors", *J. Sensors*, **2016,** 8 pages.

Li, T., Shi, C., Tan, Y., Li, R., Zhou, Z. and Ren, H. (2017), "A diaphragm type fiber Bragg grating vibration sensor based on transverse property of optical fiber with temperature compensation", *IEEE Sensors J.*, **17**(4), 1021-1029.

Li, T., Tan, Y., Han, X., Zheng, K. and Zhou, Z. (2017), "Diaphragm based fiber Bragg grating acceleration sensor with temperature compensation", *Sensors*, **17**(1), 218.

Mita, A. and Yokoi, I. (2000), "Fiber Bragg grating accelerometer for structural health monitoring", *Proceedings of the 5th International Conference on Motion and Vibration Control 2000*, Sydney, Australia, December.

Todd, M.D., Johnson, G.A., Althouse, B.A. and Vohra, S.T. (1998), "Flexural beam-based fiber Bragg grating accelerometers", *IEEE Photonics Technol. Lett.*, **10**(11), 1605-1607.

Wang, C., Lu, Q. and Cheng, L. (2013), "Novel type of temperature self-compensating acceleration transducer based on OFBG", *IEEE Sensors J.*, **13**(8), 3012-3013.

Weng, Y., Qiao, X., Feng, Z., et al. (2011), "Compact FBG diaphragm accelerometer based on L-Shaped rigid cantilever beam", *Chinese Optics Lett.*, **10**(9), (100604-1)-(100604-4).

Wu, J., Masek, V. and Cada, M. (2009), "The possible use of fiber Bragg grating based accelerometers for seismic measurements", *Proceedings of the IEEE CCECE 2009*, St. John's, Canada, May.

Xiang, L., Jiang, Q., Li, Y., and Song, R. (2016), "Design and experimental research on cantilever accelerometer based on fiber Bragg grating", *Opt. Eng.*, **55**(6), 066113.

Zhang, W., Wu, Z., Liu, Y., Yang, Y., Kai, G., Zhao, Q., et al. (2005). "Principles and realizations of FBG wavelength tuning with elastic beams", *Optoelectronic Lett.*, **1**(1), 5-9.

HJ